

GSK-3 inhibition modulates metalloproteases in a model of lung inflammation and fibrosis

Francesco Cinetto¹, Ilaria Caputo¹, Daniela Cangiano¹, Barbara Montini², Francesca Lunardi³, Carlo Agostini^{4, 1}, Fiorella Calabrese³, Gianpietro Semenzato¹, Marcello Rattazzi^{1, 5}, Carmela Gurrieri⁶, Riccardo Scarpa^{5, 7}, Jessica Ceccato¹, Fabrizio Vianello^{6, 8*}

¹Dipartimento di Medicina, Scuola di Medicina e Chirurgia, Università degli Studi di Padova, Italy,

²Pediatric Research Institute, Città della Speranza Foundation, Italy, ³Department of Cardiac, Thoracic and Vascular Sciences, School of Medicine and Surgery, University of Padua, Italy, ⁴University of Padua, Italy, ⁵Ca' Foncello Hospital, Italy, ⁶University Hospital of Padua, Italy, ⁷Other, Italy, ⁸Other, Italy

Submitted to Journal:

Frontiers in Molecular Biosciences

Specialty Section:

Molecular Diagnostics and Therapeutics

Article type:

Original Research Article

Manuscript ID:

633054

Received on:

24 Nov 2020

Frontiers website link:

www.frontiersin.org

Conflict of interest statement

The authors declare that the research was conducted in the absence of any commercial or financial relationships that could be construed as a potential conflict of interest

Author contribution statement

CA and FC conceived the study. BM, DC, IC, JC and RS conducted the experiments. FC conducted the in-vivo experiments. FC and FL performed the immunohistochemical analysis. FC and FV wrote the manuscript. GS and MR conducted the statistical analysis and revised the manuscript. RS All authors contributed to the article and approved the submitted version.

Keywords

Idiopathic lung fibrosis, Metalloproteases, Glycogen Synthase Kinase 3, bleomycin-induced lung injury, extracellular matrix (ECM)

Abstract

Word count: 277

Idiopathic Pulmonary Fibrosis (IPF) is mainly characterized by an aberrant extracellular matrix deposition, consequent to epithelial lung injury and myofibroblast activation, and inflammatory response. Glycogen Synthase Kinase 3 (GSK-3) is a serine-threonine kinase involved in several pathways and its inhibition has been already suggested as a therapeutic strategy for IPF patients. The aim of our study was to investigate the role of this kinase in the modulation of matrix metalloproteinases (MMP) -9 and -2 and their inhibitors as they are responsible for extracellular matrix turnover and therefore unbalanced in IPF pathogenesis.

C57BL/6N mice were used as in vivo model and treated with Bleomycin and or GSK-3 inhibitor, SB216763. The lungs from different animals were processed for immunohistochemical and biochemical studies or bronchoalveolar lavage. MRC5 and primary fibroblasts from IPF patients were used as the in vitro model, pre-treated with SB216763 and stimulated with TNF α or TGF β as pro-inflammatory or pro-fibrotic stimuli respectively. Western Blot and Zymographic analysis were performed. Data were statistically analysed by Student t-test.

GSK-3 inhibition modulates gelatinases activity both in mice model and cultured fibroblasts, reduces gene expression of MMP9 ($p < 0,01$), MMP2 ($p < 0,05$), TIMP1 ($p < 0,01$) and TIMP2 ($p < 0,01$) in inflammatory cells recovered from BALFs after BLM treatment, and restores their protein levels after the overexpression induced by bleomycin. Moreover, in vitro results showed that α -SMA protein levels decreases in primary fibroblasts treated with SB216763 and stimulated with TGF β (2ng/ml) ($p < 0,05$).

Our results confirm the implication of GSK-3 in IPF pathogenesis suggesting that it might play its role by modulating MMPs expression and activity, but also pushing fibroblast towards myofibroblast phenotype and therefore enhancing ECM deposition. Thus, its inhibition could represent a possible therapeutic strategy.

Contribution to the field

Local processes following lung damage involve different cells, including lung epithelial cells, fibroblasts and immune cells, particularly resident macrophages. These cells and the released mediators may influence the microenvironment and drive it towards inflammation and tissue healing or progressive fibrosis. The balance between extracellular matrix deposition and resorption represents a key point in this setting, playing matrix metalloproteases and their tissue inhibitors a pivotal role. In this contest, the protein kinase GSK3 is involved in the regulation of inflammatory and fibrotic processes affecting different organs. We here provide evidence supporting the role of GSK-3 at the crossroad between inflammation, resolution and fibrosis. We demonstrated this through the use of bleomycin-induced lung damage mouse model and by performing in vitro experiments on epithelial cells, primary macrophages and patient derived primary lung fibroblasts. We show that GSK3 pharmacologic inhibition affects, both in vivo and in vitro, lung cells pro-inflammatory and pro-fibrotic behavior, inhibiting fibroblasts activation into myofibroblasts, modulating thus the above-mentioned regulators of extra-cellular matrix remodeling. IN conclusion, GSK-3 might thus play a key role in acute and chronic lung damage, representing a possible therapeutic target in progressive fibrotic lung diseases as Idiopathic Pulmonary Fibrosis.

Ethics statements

Studies involving animal subjects

Generated Statement: The animal study was reviewed and approved by Ethical Committee for animal experimentation of the University of Padova.

Studies involving human subjects

Generated Statement: No human studies are presented in this manuscript.

Inclusion of identifiable human data

Generated Statement: No potentially identifiable human images or data is presented in this study.

In review

Data availability statement

Generated Statement: The raw data supporting the conclusions of this article will be made available by the authors, without undue reservation.

In review

1 **GSK-3 inhibition modulates metalloproteases in a model of lung**
2 **inflammation and fibrosis**

3
4 Francesco Cinetto^{1*}, Ilaria Caputo², Daniela Cangiano², Barbara Montini³, Francesca Lunardi⁴, Carlo
5 Agostini¹, Fiorella Calabrese⁴, Gianpietro Semenzato², Marcello Rattazzi¹, Carmela Gurrieri², Riccardo
6 Scarpa¹, Jessica Ceccato², and Fabrizio Vianello².

7
8 ¹Internal Medicine and Allergology and Clinical Immunology Units, Treviso Ca' Foncello Hospital
9 Treviso, Italy.

10 ²Hematology and Clinical Immunology Unit, Department of Medicine, University of Padova, Italy;

11 ³ Institute of Pediatric Research (IRP) Città della Speranza, Padova, Italy;

12 ⁴Dept. of Cardiothoracic and Vascular Sciences, Pathology Section, University of Padova, Italy

13
14
15
16
17 *** Correspondence:**

18 Corresponding Author

19 Fabrizio Vianello, MD

20 ²Hematology and Clinical Immunology Unit,

21 Department of Medicine, University of Padova, Italy

22 Phone: +39 049 8212176

23 Email: fabrizio.vianello@unipd.it

24
25 **Keywords: Pulmonary Fibrosis; matrix metalloproteinases; Glycogen Synthase Kinase 3;**
26 **bleomycin-induced lung injury; extracellular matrix**

27

28 **Abstract.**

29 Idiopathic Pulmonary Fibrosis (IPF) is mainly characterized by an aberrant extracellular matrix
30 deposition, consequent to epithelial lung injury and myofibroblast activation, and inflammatory
31 response. Glycogen Synthase Kinase 3 (GSK-3) is a serine-threonine kinase involved in several
32 pathways and its inhibition has been already suggested as a therapeutic strategy for IPF patients. The
33 aim of our study was to investigate the role of this kinase in the modulation of matrix metalloproteinases
34 (MMP) -9 and -2 and their inhibitors as they are responsible for extracellular matrix turnover and
35 therefore unbalanced in IPF pathogenesis.

36 C57BL/6N mice were used as *in vivo* model and treated with Bleomycin and or GSK-3 inhibitor,
37 SB216763. The lungs from different animals were processed for immunohistochemical and biochemical
38 studies or bronchoalveolar lavage. MRC5 and primary fibroblasts from IPF patients were used as the *in*
39 *vitro* model, pre-treated with SB216763 and stimulated with TNF α or TGF β as pro-inflammatory or pro-
40 fibrotic stimuli respectively. Western Blot and Zymographic analysis were performed. Data were
41 statistically analysed by Student t-test.

42 GSK-3 inhibition modulates gelatinases activity both in mice model and cultured fibroblasts, reduces
43 gene expression of MMP9 (p<0,01), MMP2 (p<0,05), TIMP1 (p<0,01) and TIMP2 (p<0,01) in
44 inflammatory cells recovered from BALFs after BLM treatment, and restores their protein levels after
45 the overexpression induced by bleomycin. Moreover, *in vitro* results showed that α -SMA protein levels
46 decreases in primary fibroblasts treated with SB216763 and stimulated with TGF β (2ng/ml) (p<0,05).
47 Our results confirm the implication of GSK-3 in IPF pathogenesis suggesting that it might play its role
48 by modulating MMPs expression and activity, but also pushing fibroblast towards myofibroblast
49 phenotype and therefore enhancing ECM deposition. Thus, its inhibition could represent a possible
50 therapeutic strategy.

51

52 **1. Introduction**

53 Idiopathic pulmonary fibrosis (IPF) is characterized by an extensive lung parenchyma remodeling due to
54 the abnormal deposition of extracellular matrix (ECM) by fibroblasts and the migration of epithelial
55 cells and myofibroblasts through the disrupted basement membrane (BM) into the alveolar spaces.
56 (Selman et al., 2001)

57 In this context, matrix metalloproteinases (MMPs), a family of extracellular and Zinc-dependent
58 enzymes, are proposed to play a crucial role through their proteolytic activity. (Woessner, 1991)

59 MMP activity is regulated at multiple levels including gene transcription, extracellular activation of the
60 zymogen and inactivation by specific inhibitors referred as tissue inhibitors of metalloproteinases
61 (TIMPs). (Chakraborti et al., 2003) Accumulating evidences indicate that an imbalance between MMPs
62 and TIMPs may lead to the alteration of the ECM metabolism in a variety of pulmonary disorders,
63 including IPF, emphysema, asthma and lung carcinoma. (Hayashi et al., 1996; Selman et al., 2000; Suga
64 et al., 2000; Ramos et al., 2001; Betsuyaku et al., 1999; Russell et al., 2002; Kelly and Jarjour, 2003;
65 Urbanski et al., 1992)

66 Two gelatinases, MMP-9 (gelatinase B) and MMP-2 (gelatinase A), are of particular interest as they are
67 able to degrade the common substrates collagen type IV, the major constituent of the BM, and gelatin.
68 These two gelatinases greatly differ in transcription control, with MMP-2 constitutively expressed whilst
69 MMP-9 is induced by soluble factors such as cytokines and growth factors and by integrin-mediated
70 signaling through cell-matrix or cell-cell interactions. (Chakraborti et al., 2003; Hrabec et al., 2002; He,
71 1996) Evidence suggests that inducible MMP-9 may have multiple roles in the lung, with studies
72 implicating it in wound repair of human respiratory epithelium as well as in pathological processes
73 including alveolar bronchiolization in bleomycin-induced lung injury. (Aoudjit et al., 1998; Lemjabbar
74 et al., 1999; Buisson et al., 1996; Legrand et al., 1999)

75 We previously identified anti-inflammatory and anti-fibrotic properties of the specific inhibitor of
76 Glycogen synthase kinase-3 (GSK-3), SB216763, in a mouse model of bleomycin (BLM)-induced lung
77 inflammation and fibrosis. (Gurrieri et al., 2010) GSK-3, a pleiotropic serine threonine kinase glycogen
78 synthase kinase, is known as a crucial mediator of inflammation homeostasis and is implicated in
79 pathways controlling cell proliferation and survival. It is constitutively active and it is inhibited, rather
80 than activated, in response to stimulation of two main signalling pathways, the insulin and the
81 Wnt/ β -catenin pathways.

82 GSK-3 is also involved in TGF β 1-dependent differentiation to myofibroblasts and in epithelial-to-
83 mesenchymal transition. (Baarsma et al., 2013; Caraci et al., 2008; Kim et al., 2014)

84 In this study, we aim to investigate in-vivo and in-vitro the involvement of MMP-9 and MMP-2 and of
85 their inhibitors TIMP-1 and TIMP-2 in the development of BLM-induced fibrosing alveolitis and the
86 role of the kinase GSK-3 in modulating their expression and activity.

88 **2. Materials and Methods**

89 *2.1. Mice*

90 C57BL/6N mice obtained from Charles River, Jackson Laboratories Inc. (Milan, Italy), were used for
91 this study. Mice were housed under ethical conditions in a pathogen-free animal facility. Mice were used
92 at 12 weeks of age. All procedures were approved by local Animal Care Committee of the University of
93 Padova (Padova, Italy).

95 *2.2. Experimental protocol*

96 We used the maleimide SB216763 as a selective ATP-competitive GSK-3 inhibitor.(Coghlan et al.,
97 2000) C57BL/6N mice were randomized into four different subgroups (n = 15/group) and they received
98 saline, saline plus SB216763 (control groups), BLM plus vehicle and BLM plus SB216763. No

99 differences were detected at any level between saline and saline plus SB216763 groups and so, as
100 previously described, a single control group identified as “saline” will be presented in the results
101 paragraphs. Mice were anesthetized and treated with intra-tracheal administration of isotonic saline or
102 bleomycin sulfate (3 U/Kg) (Aventis Pharma SpA, Varese, Italy) as previously described. SB216763 (20
103 mg/Kg) (Sigma-Aldrich, St. Louis, MO) dissolved in dimethyl sulfoxide and polyethylene glycol was
104 administered intraperitoneally twice a week, as previously described. (Gurrieri et al., 2010) Mice
105 underwent bronchoalveolar lavage (BAL), were sacrificed 7 days after BLM or saline administration,
106 and lungs were then processed as previously described.(Gurrieri et al., 2010)

107

108 *2.3. Histologic examination and Histochemistry*

109 Lung tissues were formalin-fixed, paraffin-embedded and 4-5µm sections were stained with
110 Hematoxylin&Eosin (H&E), to evaluate the degree of inflammatory cell infiltration and alveolar
111 epithelial cuboidalization, and stained with Masson’s trichrome to evaluate the degree of interstitial
112 fibrosis. Then, each section was scanned at 40X magnification to identify at least 5 areas (hot spots) with
113 the largest extension of fibrosis (Trichrome staining). Each hot spot was then examined at X 200
114 magnification (0.949 mm²/field) and the fibrosis was quantified by using digital quantitative analysis
115 (Image Pro Plus software version 4.1, Media Cybernetics, Silver Spring MD). The mean value of the
116 five areas was taken as representative of the whole section.

117 For immunohistochemical analyses, following dewaxing and hydration, sections were incubated in
118 citrate buffer 5 mM at pH 6.0 in a microwave oven for 30 min for antigen retrieval. Afterwards, sections
119 were treated with blocking serum (Ultratech HRP Kit; Immunotech, Beckman Coulter, USA) and
120 incubated for 60 min with the mouse monoclonal antibodies anti-MMP2, MMP-9, TIMP1, TIMP2
121 (Santa Cruz Biotechnology, CA) at a concentration of 1:200, 1:800, 1:200 and 1:500 respectively.
122 Sections were subsequently incubated with a secondary biotinylated antibody for 10 min and then with

123 streptavidin-biotin complex conjugated to horseradish peroxidase for 10 min (Ultratech HRP Kit;
124 Immunotech, Beckman Coulter). Immunoreactivity was visualised with diaminobenzidine (DAB; Dako,
125 Denmark). Finally, the sections were counterstained with Mayer's haematoxylin. Negative controls for
126 non-specific binding were processed omitting the primary antibodies and revealed no signal. The
127 expression of these markers was quantified by using a 0-3 score system and distinguishing macrophages
128 and metaplastic epithelial cells (0, no staining; 1, less than 30% of positive cells; 2, 30-60% of positive
129 cells; 3, more than 60% of positive cells).

130

131 *2.4. Bronchoalveolar Lavage (BAL) and cell count in BAL fluid (BALF)*

132 Airways were lavaged three times with 0.4 ml of sterile saline. BAL was centrifuged and supernatant
133 was stored at -80°C for the zymographic analysis. BAL cells were adjusted to the final concentration of
134 1×10^6 cells/mL in phosphate buffer saline and total cell counts were performed by manual counting
135 under light microscopy with a standard haemocytometer chamber. Finally, 100 μ L of BAL cells were
136 smeared on a glass slide and then stained with May-Grünwald Giemsa dyes. Differential counts on 200
137 cells were made using standard morphological criteria.

138

139 *2.5. Gelatin Zymography*

140 Aliquots of BAL fluid were mixed with 4X non reducing sample buffer (1,25M Tris-HCL pH 6.8, 10%
141 (w/v) sodium dodecyl sulfate (SDS), 40% (v/v) glycerol, 1% bromophenol blue) (3:1, v/v) and
142 electrophoresed on 8% SDS-PAGE containing 1% gelatin (Sigma-Aldrich, St. Louis, MO) as MMP-9
143 and MMP-2 substrate. Following electrophoresis the gels were washed twice with 2.5% Triton X-100
144 and then incubated overnight at 37°C in developing buffer (50mM Tris-based, 200mM NaCl, 10mM
145 CaCl_2 , pH 7.4). The gels were stained with 0.5% (w/v) Coumassie Brilliant Blue R-250 (Sigma-Aldrich,
146 St. Louis, MO) in 30% methanol and 10% acetic acid and destained in a solution of 30% methanol and

147 10% acetic acid. Gelatinases appear as clear bands against blue background, with recombinant protein
148 molecular weight markers used to identify the weights of the gelatinolytic bands). Relative enzyme
149 amounts were quantified by measuring the intensity of the bands with the pixel-based densitometer
150 program Quantity One®, 1-D Analysis Software (Bio-Rad Laboratories, Inc., Hercules CA). For cell
151 culture studies, cell culture supernatant media were collected and concentrated by AmiconUltra 3K
152 (Merck Millipore KGaA, Darmstadt, Germany) prior to zymography. Densitometry for cell lines
153 zymography were performed with ImageLab (Bio-Rad Laboratories, Inc., Hercules CA).

154

155 *2.6. Cell lines and treatments*

156 MRC5 cells (CCL-171, purchased by ATCC) were cultured in Dulbecco's Modified Eagle Medium
157 w/L-Glutamine (1%) w/Sodium Pyruvate (1%) w/Non essential aminoacids (1%) (Euroclone, Milan,
158 Italy) supplemented with Penicillin-Streptomycin (1%) (Euroclone, Milan, Italy), and 10% v/v Fetal
159 Bovine Serum (FBS) (Euroclone, Milan, Italy). A549 cell line (CCL-185, purchased by ATCC) were
160 cultured in the same conditions as MRC5 cells, but w/o Sodium Pyruvate.

161 Primary lung fibroblasts were isolated both from IPF and non-IPF patients. Human Primary fibroblast
162 (kindly provided by Donna E. Davies, the Brooke Laboratory, University of Southampton,
163 Southampton, UK) were isolated as previously described.(Conforti et al., 2017) All primary fibroblasts
164 were used for experiments between passages 3-6.

165 Primary monocytes were isolated from healthy buffy-coats exploiting their ability to grow attached to
166 the plate. Briefly, monocytes underwent gradient separation by using Lymphosep (Biowest, Nuaille -
167 France) before and then Percoll (GE Healthcare BioScience Ab, Uppsala, Denmark). Cells were than
168 counted and plated in a six well plate at the density of 2×10^6 cells/well. After 1h, floating cells were
169 discarded and only attached cells (monocytes) were treated with GM-CSF (Miltenyi Biotec, Bologna,

170 Italy) in order to push monocytes toward an M0 - like phenotype (Del Prete et al., 1995). After 7 days,
171 GM-CSF was removed and treatments have been performed, as described later.

172 Proliferative cultures (for every cell lines) were incubated at 37°C in a humidified 5% CO₂ incubator
173 and subculture carried out by washing the cell monolayers twice with calcium and magnesium-free
174 Dulbecco phosphate buffered saline (DPBS) (Euroclone, Milan, Italy), followed by addition of 1X
175 Trypsin/ EDTA solution (Gibco, Thermofisher, Monza, Italy) and incubation at 37°C until the cells
176 detached. Cells were seeded (1,5-2x10⁵ cells/well), using six well plates.

177 Cells (fibroblasts, alveolar epithelial cells and monocytes/macrophages-derived cells) were starved and
178 treated with TNF α (Sigma-Aldrich, St. Louis, MO) at the concentration of 15 ng/ml or TGF β
179 (PeproTech, London, UK) at 2-5 ng/ml, in presence or absence of SB216763 (Sigma-Aldrich, St. Louis,
180 MO), an inhibitor of GSK-3, used at the concentration of 8 μ M for A549 and . 10 μ M for fibroblasts and
181 macrophages, on the basis of what reported in literature and of our preliminary data. Experiments were
182 performed both for 24 and 48 hours in complete serum starvation.

183

184 2.7. *Western Blot*

185 After 24 and 48 hours of stimulation with TNF α or TGF β , proteins were extracted with tissue protein
186 extraction reagent (Santa Cruz, CA, USA) with the addition of a protease inhibitor (Roche, Basel,
187 Switzerland). The concentration was then measured using the Bradford quantification assay (Pierce,
188 Thermo Scientific, Rockford, IL). Equal amounts of proteins (10 μ g) were denatured in Laemli buffer
189 (Bio-Rad Laboratories, Inc., Hercules CA) added with β -mercaptoethanol (Sigma-Aldrich, St. Louis,
190 MO). Samples were boiled for 4 minutes, separated by 10% SDS-PAGE gel, and electrophoretically
191 transferred onto PVDF membranes (Thermo Scientific, Rockford, IL). The membranes were blocked for

192 1h at room temperature with 5% not-fat dry milk in TBS added with 0.1% Tween-20 (Sigma-Aldrich,
193 St. Louis, MO), followed by overnight incubation at 4°C with the following antibodies: MMP-9 (Merck
194 Millipore KGaA, Darmstadt, Germany); MMP2 (Merck Millipore KGaA, Darmstadt, Germany); TIMP1
195 (Abcam, Cambridge, USA); TIMP2 (Abcam, Cambridge, USA); α SMA (Sigma-Aldrich, St. Louis,
196 MO); GAPDH (Merck Millipore KGaA, Darmstadt, Germany).

197 *2.8. Real-time PCR amplification*

198 mRNA was extracted from BALF inflammatory cells using TRIzol reagent (Invitrogen Life
199 Technologies, Grand Island, NY) and reversed transcribed into cDNA using Reverse Transcription
200 System (PROMEGA, Madison, WI) according to the manufacturer's instructions. Real-time PCR
201 amplification was performed on an ABI PRISM 7000 sequence detection system (Applied Biosystems,
202 Foster City, CA). Reactions were carried out with Platinum[®] SYBR[®] Green qPCR SuperMix-UDG kit
203 (Invitrogen Life Technologies, Carlsbad, CA). Primer sequences were reported in Table 1. β -actin was
204 used as housekeeping gene. Data were first calculated as mean of the ratio of the target mRNA to that of
205 β -actin and subsequently normalized to the control group.

206

207 *2.9. Statistical analysis*

208 All data are expressed as means \pm Standard Deviation (SD). Statistical differences among groups were
209 determined using Student's t-test. Significance was defined at the $p < 0,05$. Analysis and graphs were
210 realized using GraphPad Prism 7.0 (GraphPad Software, Inc., San Diego, CA).

211

212

213

214

215

216

217

218

219

220

221 **3. RESULTS**

222 *3.1. BALF cell composition*

223 We previously demonstrated that the intratracheal administration of BLM induced pulmonary alveolitis
224 peaking at day + 7 (Gurrieri et al., 2010). We performed total cell count of BALF recovered at day + 7
225 from mice of each experimental group and we found that total cell number significantly increased in
226 BLM-instilled mice compared to control mice instilled with saline ($p < 0.05$; Table 2). Moreover, the co-
227 treatment of BLM-instilled mice with SB216763 significantly reduced total cell number of the BALF (p
228 < 0.05 ; Table 2) confirming our previous findings. (Gurrieri et al., 2010) When evaluating BALF cell
229 composition, macrophages represented the main cell population in control mice, as expected; in contrast,
230 mice exposed to BLM showed a strong increase of lymphocyte percentage as well as the detectability of
231 the two sub-populations of neutrophils and eosinophils. The inhibition of GSK-3 with SB216763
232 significantly reduced the lymphocyte percentage ($p < 0.01$), with a recovery of the physiological
233 percentage of macrophages (Table 2). This finding was in accordance with our previously published data
234 of flow cytometric analysis, showing how the inhibition of GSK-3 induced a reduction in CD3⁺ T
235 lymphocyte percentage at day + 7. (Gurrieri et al., 2010) An observed reduction of neutrophil and
236 eosinophil percentage was not statistically significant.

237

238 *3.2. BLM-induced MMP-9 and MMP-2 activity is modulated following GSK-3 inhibition*

239 We next performed gelatin zymography to detect MMP-9 and MMP-2 gelatinolytic activity of
240 BALF supernatant. Control mice (saline or saline plus SB216763) showed very low gelatinolytic
241 activity. In contrast, the instillation of mice with BLM increased MMP-9 activity at day 7 and the
242 zymographic analysis showed two distinct bands at 105 KDa and 125 KDa corresponding to pro-MMP-
243 9 and MMP-9/neutrophil gelatinase-associated lipocalin complex (NGAL), respectively (Fig.1b).
244 Moreover, SB216763 treatment of mice exposed to BLM broke down the NGAL/MMP-9 complex and
245 strongly reduced the latent form of MMP-9 (Fig.1b). The densitometric analysis indicated that pro-
246 MMP-9 levels of SB216763-treated mice decreased 10 times compared to those of mice given only
247 BLM ($p < 0.001$) (Fig.1a).
248 Zymographic analysis for MMP-2 revealed two gelatinolytic bands corresponding to the active (52
249 KDa) and the latent form (72 KDa) in mice treated with BLM (Fig. 1c). In this setting, GSK-3 inhibitor
250 showed a lower but significant modulation of MMP-2 activity, with a reduction ($p < 0.05$) for active-
251 MMP-2 and pro-MMP2 compared to BLM-treated mice (Fig. 1 d,e).

252

253

254 3.3. Gene expression analysis of MMP-9 and MMP-2 in BALF cells.

255 Next, we quantified MMP-9 and MMP-2 transcript levels in the cells recovered from BALFs of
256 mice. Mice instilled with BLM showed a very strong increase of MMP-9 gene expression compared
257 with control mice ($p < 0.01$). The co-treatment of the mice with BLM plus SB216763 reduced MMP-9
258 mRNA levels to the normal levels of the control group ($p < 0.01$) (Fig. 2a). Similarly, we observed the
259 increase of MMP-2 gene expression in BLM-treated mice compared to control mice ($p < 0.05$) and that
260 SB216763 co-administered with BLM reduced the augmented MMP-2 mRNA levels ($p < 0.05$) (Fig. 2b)

261 Then, we assessed gene-expression levels of TIMP-1 and TIMP-2, the physiologic inhibitors of
262 MMP-9 and MMP-2 respectively. Although both transcripts were detected at low levels in inflammatory

263 cells collected from BALFs, we found that TIMP-1 and TIMP-2 expression was augmented in BLM-
264 treated mice compared to control mice ($p < 0.01$) and the inhibition of GSK-3 reduced the mRNA levels
265 to the values of the control group ($p < 0.01$) (Fig. 2 c,d).

266

267 *3.4. GSK-3 inhibition downmodulates MMP-9, TIMP-1, MMP-2 and TIMP-2 overexpression induced by*
268 *BLM in interstitial alveolar macrophages and cuboidalized epithelial alveolar cells.*

269 Immunohistochemistry was performed in all mouse lung samples in order to correlate tissue expression
270 of MMPs and TIMPs to that observed in BALF. iAMs, the main cell population infiltrating lung
271 interstitium at this time point, showed a strong staining for MMP-9 ($80 \pm 8.7\%$), TIMP-1 ($78 \pm 4.6\%$), and
272 MMP-2 ($66 \pm 14\%$) and were moderately positive for TIMP-2 ($55 \pm 28\%$) at day 7 after BLM instillation
273 (Fig. 3). *In vivo* SB216763 co- treatment moderately reduced iAM staining for MMP-9 ($50 \pm 24\%$) and
274 markedly down-modulated TIMP-1 ($32 \pm 26\%$) and TIMP-2 ($22 \pm 18\%$) positivity. MMP-2 expression,
275 instead, was not significantly affected by GSK-3 inhibition (Fig. 3).

276 When focusing on the metaplastic cuboidalized type II epithelial alveolar cells, a positive staining for
277 MMP-2 ($23.3 \pm 16.3\%$), MMP-9 ($28.5 \pm 22\%$), TIMP-1 ($22 \pm 16\%$), and TIMP-2 ($15 \pm 17\%$), was detected
278 after BLM administration. Interestingly a consistent reduction of MMP-9 and MMP-2 staining in
279 cuboidalized type II epithelial alveolar cells followed co-treatment with SB216763 (from 28.5 to 4.3%
280 and from 23.3 to 1.67%, respectively, at day 7; $p < 0.05$ - Fig. 4). Moreover, no epithelial staining for
281 TIMP-1 and TIMP-2 was detectable in SB216763-treated group (Fig. 4).

282 *3.5. MMP pattern In Vitro*

283 Starting from the *in vivo* evidence of the role of epithelial alveolar cells and macrophages in MMPs and
284 TIMPs production, we performed *in vitro* experiments using the same human cell types: epithelial
285 alveolar type II cells (A549) and human primary monocytes/macrophages. We also used human lung

286 fibroblasts (MRC5 cell line and primary IPF fibroblasts), since they are known to be involved in ECM
287 turnover in IPF pathogenesis

288 At first, to confirm in vitro the functional properties of SB216763, we measured β -catenin expression in
289 epithelial alveolar type II cells (A549) after exposure to SB216763 by Western blot analysis. β -catenin
290 is a direct phosphorylation target of GSK3 and inhibition of GSK3 results in decreased phosphorylation
291 and stabilization of β -catenin (Schmid et al., 2017; Cross et al., 2001; Wang et al., 2015). As expected,
292 the expression of β -catenin was significantly increased (mean values 1,25, 1,62 and 2,27 at 1, 4 and 8
293 mM SB216763 concentration, respectively) in treated compared to untreated cells (data not shown).
294 Similar results were obtained with the other cell types. In our further experiments with A549 cells, GSK-
295 3 inhibition by SB216763 did not significantly affect MMPs and TIMPs production downstream of
296 $\text{TNF}\alpha$ and $\text{TGF}\beta$ stimulation (data not shown).

297

298 *3.6. GSK-3 inhibition by SB216763 modulates MMPs activity in pulmonary fibroblasts*

299 MRC5 cells and primary IPF fibroblasts were treated with $\text{TNF}\alpha$ or different concentration of $\text{TGF}\beta$ as
300 above detailed. Supernatant were collected and underwent zymographic analysis. Our results show that,
301 in MRC5 cells, MMP9 activity significantly decreased upon $\text{TGF}\beta$ stimulation in presence of GSK-3
302 inhibitor, with statistical significance observed at 2 ng/ml concentration (Fig. 5a). Moreover, the pro-
303 form of MMP2 significantly decreased at both concentration of $\text{TGF}\beta$ after pre-treatment with
304 SB216763 (Fig. 5b) at 24 h, with no increase of the active form. No significant differences were
305 observed at 48 h (data not shown). $\text{TGF}\beta$ and $\text{TNF}\alpha$ stimulation of IPF primary fibroblasts did not affect
306 MMP9 and MMP2 activity, and no effect of GSK-3 inhibition was observed (figure 5 c-d).

307

308 *3.7. SB216763 decreases α -SMA protein levels upon pro-fibrotic stimulation*

309 In IPF pathogenesis, the differentiation of fibroblasts to myofibroblasts further enhances the ECM
310 aberrant deposition. Therefore, we also studied the expression of α SMA as a marker of this transition
311 using primary IPF fibroblasts and MRC5 cells. As expected from literature (Baarsma et al., 2013), our
312 data confirmed that α SMA protein levels increase downstream of TGF β stimulation; co-treatment with
313 SB216763 decreased these levels at 48h, reaching statistical significance at 2 ng/ml TGF β concentration
314 ($p < 0,05$) in primary fibroblasts (Fig. 6). Consistent with our IPF fibroblast studies, α SMA protein levels
315 in MRC5 cells increased after TGF β stimulation and decreased after co-treatment with SB216763,
316 although the decrease did not reach statistical significance (data not shown).

317 3.8. GSK-3 inhibition by SB216763 modulates MMP2 protein expression in primary 318 monocytes/macrophages

319 As we observed a role for macrophages in the inflammatory response in our *in vivo* studies, we then
320 investigated whether GSK-3 inhibition modulated MMPs protein expression also *in vitro*. GSK-3
321 inhibition significantly reduced Pro- and Active MMP2 protein levels ($p < 0,05$) upon TGF β stimulation
322 whilst TNF α stimulation induced an increase in MMP2 protein expression, with SB216763 pre-
323 treatment decreasing MMP-2 levels ($p < 0.05$) (Fig. 7). Finally, gelatin zymography performed on
324 macrophages supernatant did not show significant differences in activity.

325

326 4. Discussion

327 We previously demonstrated an anti-inflammatory and anti-fibrotic effect of GSK-3 inhibition in a
328 mouse model of BLM-induced pulmonary fibrosis. (Gurrieri et al., 2010) In the present study we further
329 investigated the role of GSK-3 in ECM remodelling, which is known to play a pivotal role in IPF,
330 focusing upon the modulation of MMPs and TIMPs which are essential in the physiological turnover of
331 the matrix and in the repair of disrupted BM.

332 Our *in vivo* studies used the BLM-induced mouse model of lung inflammation and fibrosis that, with all
333 known limitations, is still the most used *in vivo* approach for studying IPF pathogenesis as well as
334 potential anti-fibrotic drugs before phase I clinical trials. (Scotton et al., 2013; Craig et al., 2015)

335 We found that MMP-2, MMP-9 and TIMP-1 and TIMP-2 levels were increased in BALF of BLM
336 treated mice, and we provided evidences that iAMs are, at least in part, responsible for the release of
337 these mediators. We also demonstrated that SB216763-mediated GSK-3 inhibition strongly decreased
338 MMP-9 activity and, to a lower extent, MMP-2 activity in BALF of BLM-treated mice. Moreover,
339 SB216763 significantly reduced MMP-9, MMP-2, TIMP-1 and TIMP-2 production in iAMs and
340 cuboidalized type II epithelial alveolar cells at day 7. Consistent with our findings, it has previously
341 been demonstrated in studies of dendritic spinal plasticity that increasing GSK-3 β activity increases
342 MMP-9 activity and that nonspecific GSK-3 β inhibitor lithium is effective in down-regulating this
343 metalloprotease (Kondratiuk et al., 2017).

344 Current understanding of the role of MMPs in IPF derive from expression levels in blood, BALF and
345 lung samples of patients with IPF and from mouse studies of MMP gene-targeted mice. (Craig et al.,
346 2015)

347 Betsuyaku et al. found that fibrosing alveolitis develops in MMP-9-deficient mice after intratracheal
348 bleomycin, irrespective of MMP-9. (Betsuyaku et al., 2000) However, MMP-9 facilitates migration of
349 Clara cells into the regions of alveolar injury, thus favouring alveolar bronchiolization. At the same
350 extent, patients with IPF showed increased production of matrix metalloproteinase -8 and -9 in the
351 airways without a compensatory increase of TIMPs, suggesting that enhanced activity of MMPs may
352 contribute to matrix disruption and remodelling in the development of fibrosis. Moreover, *in vivo* use of
353 the MMP inhibitor Batimastat has been shown to inhibit MMPs thus preventing BLM-induced
354 pulmonary fibrosis. (Corbel et al., 2001)

355 The role of MMP-2 in IPF pathogenesis is less defined. MMP-2 expression is increased in IPF lungs
356 mainly in reactive airway epithelial cells and myofibroblasts. (Fukuda et al., 1998) Of importance, by
357 inducing targeted proteolysis of the BM, MMP2 has been shown to promote EMT, with loss of epithelial
358 features and acquisition of a mesenchymal phenotype.

359

360 Our BALF data combined with IHC results show that GSK-3 inhibition is effective in modulation of
361 MMP2 and MMP9 and that macrophages and cuboidalized epithelial alveolar cells might act as the main
362 characters of the play. However, whether SB216763 directly modulates MMP or it acts indirectly
363 through an anti-inflammatory effect cannot be addressed in the mouse model. To address this question
364 and further understand the molecular mechanisms underlying the role of GSK-3 in MMPs modulation,
365 we then performed in vitro studies. There is evidence that MMP9 can be activated directly from MMP2
366 and that its expression can be modulated by GSK-3 downstream c-Myc in oral squamous carcinoma
367 cells. (Pramanik et al., 2018) It has also been shown that inhibition of GSK-3 down-regulates the
368 expression of MMP2 and MT1-MMP in glioblastoma cells and that MMP2 activation is mediated by the
369 interaction of its pro-form with another metalloprotease, MT1-MMP, and TIMP2. (Chikano et al., 2015;
370 Hernandez-Barrantes et al., 2000) Surprisingly, in the A549 epithelial cell line, we found discrepancies
371 between in-vitro and in-vivo effects of GSK-3 inhibition on MMPs modulation following pro-
372 inflammatory and pro-fibrotic stimulation. In fact, we could not confirm the strong reduction in MMPs
373 expression observed in mice after SB21 treatment as GSK-3 inhibition did not affect MMPs protein
374 expression in the A549 cell line. This is likely due to a limitation of our study, since we had no chance to
375 use primary epithelial alveolar type II cells and we only tested our hypothesis using the A549 epithelial
376 cell line which is derived from *non small cell lung cancer* tissue, a type of cancer where GSK-3 is
377 known to be activated and involved in neoplastic proliferation and has been recently suggested as a
378 potential therapeutic target. (O'Flaherty et al., 2019; Xie et al., 2018)

379

380 Moving to lung fibroblasts, we then identified that MRC5 and primary IPF cells behaved differently in
381 terms of MMPs modulation. Indeed, MMP9 protein levels were unaffected by SB216763 treatment in
382 both cell types but, interestingly, GSK-3 inhibition down-modulated MMP9 activity in MRC5 cells upon
383 TGF β stimulation while producing no effect in IPF primary fibroblasts. At the same time, TGF β -
384 induced pro-MMP2 activity also decreased in MRC5 cells after pre-treatment with SB216763 but no
385 significant modification has been observed in IPF cells under the same conditions. Additionally, we
386 demonstrated that GSK-3 inhibition significantly decreases α SMA protein levels in primary human IPF
387 lung fibroblasts, upon TGF β stimulation. The same effect was not observed in MRC5 lung fibroblasts.
388 Increase in α SMA protein expression by fibroblasts is a well-known marker of fibroblasts-to-
389 myofibroblasts (F-to-MF) transition.

390 Myofibroblasts are fundamental in restoring tissue integrity after wound healing by regulating
391 the normal fibrotic process. However, myofibroblasts sustained presence stimulates dysfunctional repair
392 mechanisms, causing excess contraction, extracellular matrix secretion, and thus, fibrosis. (Klingberg et
393 al., 2013)

394 Our results confirm the potential role of GSK-3 inhibition in preventing fibroblasts-to-myofibroblasts
395 transition upon TGF β stimulation, particularly in IPF primary fibroblasts. This is in agreement with
396 previous data demonstrating an effect of GSK-3 inhibition in decreasing α SMA protein levels in primary
397 human lung fibroblasts, mediated by CREB phosphorylation.(Baarsma et al., 2013) On the contrary,
398 other researchers highlighted an opposite effect of GSK-3 inhibition on F-to-MF, mediated by β -catenin
399 pathway. (Caraci et al., 2008) This is likely due to differences in cell types, adopted concentration of
400 TGF β and different ways of GSK-3.

401 According to our results, GSK-3 inhibition may thus induce an anti-fibrotic effect, by preventing F-to
402 MF transition, as suggested by the decrease in α SMA expression. Whether the effect of GSK-inhibition
403 on MMPs and TIMPs modulation, in this context, depends on a direct regulation or simply on a
404 reduction in myofibroblasts differentiation, still needs to be investigated.

405 Our results from primary macrophages confirm that alveolar macrophages might also be a relevant
406 target for GSK-3 inhibition, as suggested by IHC analysis on the mouse model. Macrophages are indeed
407 sensitive both to the pro-inflammatory (TNF α) and the pro-fibrotic (TGF β) stimulation, overlapping at
408 day 7 after bleomycin-induced lung damage, and GSK-3 pharmacologic inhibition impacts on MMP2
409 expression upon both stimuli. Due to their role in wound healing, the implication of macrophages and
410 their environmental modulatory function in the pathogenesis of pulmonary fibrosis is still under
411 investigation. (Zhang et al., 2018)

412
413 Finally, our *in vivo* results may be relevant when considering whether inhibition rather than complete
414 silencing of GSK-3 would be the optimal pharmacologic strategy. GSK-3 is a pleiotropic kinase
415 implicated in many different pathways. It has been shown that GSK-3 β knockout mice are
416 embryonically lethal. (Hoefflich et al., 2000) On the other hand, the long clinical experience with lithium
417 teaches us that *in vivo* inhibition of this kinase is safe and effective. This is likely due to the partial
418 inhibition that lithium exerts on GSK-3, which may be optimal for dampening GSK-3's self-activating
419 mechanisms in pathologic processes while allowing GSK-3 to exert, unhampered, its many other cellular
420 actions. (Beurel et al., 2015) Thus, it is not surprising that *in vitro* single cell culture experiments
421 provide more uncertainties and discrepancies than *in vivo* results, suggesting that a more complex
422 environment should be generated to obtain trustable *in vitro* results. This is further testified by the
423 different behaviours highlighted between MRC5 fibroblast cell line and primary IPF fibroblasts under

424 the same culture and stimulation conditions, likely due to the pathologic context from which primary
425 cells had been isolated bearing a sort of “environmental signature” . With this consideration, the
426 pharmacologic in vivo inhibition performed in our mouse model might be not only closer to the possible
427 application in clinical practice, but also more suitable than in vitro experiments to really assess the role
428 of the kinase and the actual potential of its inhibition. In addition to the potential benefit of only partial
429 inhibition of GSK-3, in terms of future applications, the development of disease-selective inhibition
430 strategy of GSK-3 will hopefully be possible, based on the awareness of the specific mechanisms that
431 regulate GSK-3 and that depend on GSK-3 in the specific pathologic context.

432 In conclusion, our in vivo studies showed that GSK3 inhibition protected mice against the BLM-
433 induced lung damage and modulates MMP-2 and -9 expression and activity in BALF and lung tissue.
434 Our in vitro experiments confirmed the effect of GSK-3 inhibition on macrophages and on fibroblasts,
435 where SB216763 showed an impact on the expression of α -SMA, a marker of fibroblasts-to-
436 myofibroblast transition. These results provide further hints about the role of GSK-3 in the pathogenesis
437 of pulmonary fibrosis, a role that still presents some controversies in the available literature (Caraci et
438 al., 2008; Baarsma et al., 2013). Due to its implications at different levels in so many pathways involved
439 in the development of fibrosis, GSK-3 remains a fascinating target in the field of IPF, where the aim of
440 the research is not to close a bad way but to disrupt a dangerous network.

441

442

443

444

445

446 **5. Acknowledgements**

447 These authors gratefully acknowledge financial support from Associazione Franco Marcolin Onlus and
448 from Monica Fedeli and Edward Taylor

449

450

451

452

453

454

455

456

457

458

459

460

461

462

463

464

465

466

467

468

In review

469 **6. References**

- 470 Aoudjit, F., Potworowski, E. F., & St-Pierre, Y. (1998). Bi-directional induction of matrix
471 metalloproteinase-9 and tissue inhibitor of matrix metalloproteinase-1 during T lymphoma/endothelial
472 cell contact: implication of ICAM-1 (Research Support, Non-U.S. Gov't). *J Immunol*, 160(6), 2967-73.
- 473 Baarsma, H. A., Engelbertink, L. H., van Hees, L. J., Menzen, M. H., Meurs, H., Timens, W., et al. (2013).
474 Glycogen synthase kinase-3 (GSK-3) regulates TGF-beta(1)-induced differentiation of pulmonary
475 fibroblasts. *Br J Pharmacol*, 169(3), 590-603. doi:10.1111/bph.12098.
- 476 Betsuyaku, T., Fukuda, Y., Parks, W. C., Shipley, J. M., & Senior, R. M. (2000). Gelatinase B is required
477 for alveolar bronchiolization after intratracheal bleomycin (Research Support, Non-U.S. Gov't
478 Research Support, U.S. Gov't, P.H.S.). *Am J Pathol*, 157(2), 525-35. doi:10.1016/S0002-9440(10)64563-
479 4.
- 480 Betsuyaku, T., Nishimura, M., Takeyabu, K., Tanino, M., Venge, P., Xu, S., et al. (1999). Neutrophil
481 granule proteins in bronchoalveolar lavage fluid from subjects with subclinical emphysema (Research
482 Support, Non-U.S. Gov't). *Am J Respir Crit Care Med*, 159(6), 1985-91.
483 doi:10.1164/ajrccm.159.6.9809043.
- 484 Beurel, E., Grieco, S. F., & Jope, R. S. (2015). Glycogen synthase kinase-3 (GSK3): regulation, actions,
485 and diseases. *Pharmacol Ther*, 148, 114-31. doi:10.1016/j.pharmthera.2014.11.016.
- 486 Buisson, A. C., Zahm, J. M., Polette, M., Pierrot, D., Bellon, G., Puchelle, E., et al. (1996). Gelatinase B
487 is involved in the in vitro wound repair of human respiratory epithelium (Research Support, Non-U.S.
488 Gov't). *J Cell Physiol*, 166(2), 413-26. doi:10.1002/(SICI)1097-4652(199602)166:2<413::AID-
489 JCP20>3.0.CO;2-A.
- 490 Caraci, F., Gili, E., Calafiore, M., Failla, M., La Rosa, C., Crimi, N., et al. (2008). TGF-beta1 targets the
491 GSK-3beta/beta-catenin pathway via ERK activation in the transition of human lung fibroblasts into
492 myofibroblasts. *Pharmacol Res*, 57(4), 274-82. doi:10.1016/j.phrs.2008.02.001.

493 Chakraborti, S., Mandal, M., Das, S., Mandal, A., & Chakraborti, T. (2003). Regulation of matrix
494 metalloproteinases: an overview (Research Support, Non-U.S. Gov't
495 Review). *Mol Cell Biochem*, 253(1-2), 269-85.

496 Chikano, Y., Domoto, T., Furuta, T., Sabit, H., Kitano-Tamura, A., Pyko, I. V., et al. (2015). Glycogen
497 synthase kinase 3 β sustains invasion of glioblastoma via the focal adhesion kinase, Rac1, and c-Jun N-
498 terminal kinase-mediated pathway. *Mol Cancer Ther*, 14(2), 564-74. doi:10.1158/1535-7163.MCT-14-
499 0479.

500 Coghlan, M. P., Culbert, A. A., Cross, D. A., Corcoran, S. L., Yates, J. W., Pearce, N. J., et al. (2000).
501 Selective small molecule inhibitors of glycogen synthase kinase-3 modulate glycogen metabolism and
502 gene transcription. *Chem Biol*, 7(10), 793-803. doi:10.1016/s1074-5521(00)00025-9.

503 Conforti, F., Davies, E. R., Calderwood, C. J., Thatcher, T. H., Jones, M. G., Smart, D. E., et al. (2017).
504 The histone deacetylase inhibitor, romidepsin, as a potential treatment for pulmonary fibrosis. *Oncotarget*,
505 8(30), 48737-48754. doi:10.18632/oncotarget.17114.

506 Corbel, M., Caulet-Maugendre, S., Germain, N., Molet, S., Lagente, V., & Boichot, E. (2001). Inhibition
507 of bleomycin-induced pulmonary fibrosis in mice by the matrix metalloproteinase inhibitor batimastat. *J*
508 *Pathol*, 193(4), 538-45. doi:10.1002/path.826.

509 Craig, V. J., Zhang, L., Hagood, J. S., & Owen, C. A. (2015). Matrix metalloproteinases as therapeutic
510 targets for idiopathic pulmonary fibrosis. *Am J Respir Cell Mol Biol*, 53(5), 585-600.
511 doi:10.1165/rcmb.2015-0020TR.

512 Cross, D. A., Culbert, A. A., Chalmers, K. A., Facci, L., Skaper, S. D., & Reith, A. D. (2001). Selective
513 small-molecule inhibitors of glycogen synthase kinase-3 activity protect primary neurones from death. *J*
514 *Neurochem*, 77(1), 94-102. doi:10.1046/j.1471-4159.2001.t01-1-00251.x.

515 Del Prete, G., De Carli, M., Lammel, R. M., D'Ellos, M. M., Daniel, K. C., Giusti, B., et al. (1995). Th1
516 and Th2 T-helper cells exert opposite regulatory effects on procoagulant activity and tissue factor
517 production by human monocytes (Comparative Study
518 Research Support, Non-U.S. Gov't). *Blood*, 86(1), 250-7.

519 Fukuda, Y., Ishizaki, M., Kudoh, S., Kitaichi, M., & Yamanaka, N. (1998). Localization of matrix
520 metalloproteinases-1, -2, and -9 and tissue inhibitor of metalloproteinase-2 in interstitial lung diseases
521 (Research Support, Non-U.S. Gov't). *Lab Invest*, 78(6), 687-98.

522 Gurrieri, C., Piazza, F., Gnoato, M., Montini, B., Biasutto, L., Gattazzo, C., et al. (2010). 3-(2,4-
523 dichlorophenyl)-4-(1-methyl-1H-indol-3-yl)-1H-pyrrole-2,5-dione (SB216763), a glycogen synthase
524 kinase-3 inhibitor, displays therapeutic properties in a mouse model of pulmonary inflammation and
525 fibrosis. *J Pharmacol Exp Ther*, 332(3), 785-94. doi:10.1124/jpet.109.153049.

526 Hayashi, T., Stetler-Stevenson, W. G., Fleming, M. V., Fishback, N., Koss, M. N., Liotta, L. A., et al.
527 (1996). Immunohistochemical study of metalloproteinases and their tissue inhibitors in the lungs of
528 patients with diffuse alveolar damage and idiopathic pulmonary fibrosis. *Am J Pathol*, 149(4), 1241-56.

529 He, C. (1996). Molecular mechanism of transcriptional activation of human gelatinase B by proximal
530 promoter. *Cancer Lett*, 106(2), 185-91.

531 Hernandez-Barrantes, S., Toth, M., Bernardo, M. M., Yurkova, M., Gervasi, D. C., Raz, Y., et al. (2000).
532 Binding of active (57 kDa) membrane type 1-matrix metalloproteinase (MT1-MMP) to tissue inhibitor of
533 metalloproteinase (TIMP)-2 regulates MT1-MMP processing and pro-MMP-2 activation. *J Biol Chem*,
534 275(16), 12080-9.

535 Hoeflich, K. P., Luo, J., Rubie, E. A., Tsao, M. S., Jin, O., & Woodgett, J. R. (2000). Requirement for
536 glycogen synthase kinase-3beta in cell survival and NF-kappaB activation. *Nature*, 406(6791), 86-90.
537 doi:10.1038/35017574.

538 Hrabec, E., Streck, M., Nowak, D., Greger, J., Suwalski, M., & Hrabec, Z. (2002). Activity of type IV
539 collagenases (MMP-2 and MMP-9) in primary pulmonary carcinomas: a quantitative analysis. *J Cancer*
540 *Res Clin Oncol*, 128(4), 197-204. doi:10.1007/s00432-001-0320-3.

541 Kelly, E. A., & Jarjour, N. N. (2003). Role of matrix metalloproteinases in asthma (Research Support,
542 U.S. Gov't, P.H.S.
543 Review). *Curr Opin Pulm Med*, 9(1), 28-33.

544 Kim, E. Y., Kim, A., Kim, S. K., Kim, H. J., Chang, J., Ahn, C. M., et al. (2014). Inhibition of mTORC1
545 induces loss of E-cadherin through AKT/GSK-3 β signaling-mediated upregulation of E-cadherin
546 repressor complexes in non-small cell lung cancer cells. *Respir Res*, 15, 26. doi:10.1186/1465-9921-15-
547 26.

548 Klingberg, F., Hinz, B., & White, E. S. (2013). The myofibroblast matrix: implications for tissue repair
549 and fibrosis. *J Pathol*, 229(2), 298-309. doi:10.1002/path.4104.

550 Kondratiuk, I., Łęski, S., Urbańska, M., Biecek, P., Devijver, H., Lechat, B., et al. (2017). GSK-3 β and
551 MMP-9 Cooperate in the Control of Dendritic Spine Morphology. *Mol Neurobiol*, 54(1), 200-211.
552 doi:10.1007/s12035-015-9625-0.

553 Legrand, C., Gilles, C., Zahm, J. M., Polette, M., Buisson, A. C., Kaplan, H., et al. (1999). Airway
554 epithelial cell migration dynamics. MMP-9 role in cell-extracellular matrix remodeling (Research
555 Support, Non-U.S. Gov't). *J Cell Biol*, 146(2), 517-29.

556 Lemjabbar, H., Gosset, P., Lechapt-Zalcman, E., Franco-Montoya, M. L., Wallaert, B., Harf, A., et al.
557 (1999). Overexpression of alveolar macrophage gelatinase B (MMP-9) in patients with idiopathic
558 pulmonary fibrosis: effects of steroid and immunosuppressive treatment. *Am J Respir Cell Mol Biol*, 20(5),
559 903-13. doi:10.1165/ajrcmb.20.5.3260.

560 O'Flaherty, L., Shnyder, S. D., Cooper, P. A., Cross, S. J., Wakefield, J. G., Pardo, O. E., et al. (2019).
561 Tumor growth suppression using a combination of taxol-based therapy and GSK3 inhibition in non-small
562 cell lung cancer. *PLoS One*, 14(4), e0214610. doi:10.1371/journal.pone.0214610.

563 Pramanik, K. K., Nagini, S., Singh, A. K., Mishra, P., Kashyap, T., Nath, N., et al. (2018). Glycogen
564 synthase kinase-3 β mediated regulation of matrix metalloproteinase-9 and its involvement in oral
565 squamous cell carcinoma progression and invasion. *Cell Oncol (Dordr)*, 41(1), 47-60.
566 doi:10.1007/s13402-017-0358-0.

567 Ramos, C., Montaña, M., García-Alvarez, J., Ruiz, V., Uhal, B. D., Selman, M., et al. (2001). Fibroblasts
568 from idiopathic pulmonary fibrosis and normal lungs differ in growth rate, apoptosis, and tissue inhibitor
569 of metalloproteinases expression. *Am J Respir Cell Mol Biol*, 24(5), 591-8. doi:10.1165/ajrcmb.24.5.4333.

570 Russell, R. E., Culpitt, S. V., DeMatos, C., Donnelly, L., Smith, M., Wiggins, J., et al. (2002). Release
571 and activity of matrix metalloproteinase-9 and tissue inhibitor of metalloproteinase-1 by alveolar
572 macrophages from patients with chronic obstructive pulmonary disease (Comparative Study
573 Research Support, Non-U.S. Gov't). *Am J Respir Cell Mol Biol*, 26(5), 602-9.
574 doi:10.1165/ajrcmb.26.5.4685.

575 Schmid, A., Sailland, J., Novak, L., Baumlin, N., Fregien, N., & Salathe, M. (2017). Modulation of Wnt
576 signaling is essential for the differentiation of ciliated epithelial cells in human airways. *FEBS Lett*,
577 591(21), 3493-3506. doi:10.1002/1873-3468.12851.

578 Scotton, C. J., Hayes, B., Alexander, R., Datta, A., Forty, E. J., Mercer, P. F., et al. (2013). Ex vivo micro-
579 computed tomography analysis of bleomycin-induced lung fibrosis for preclinical drug evaluation
580 (Research Support, Non-U.S. Gov't). *Eur Respir J*, 42(6), 1633-45. doi:10.1183/09031936.00182412.

581 Selman, M., King, T. E., Pardo, A., Society, A. T., Society, E. R., & Physicians, A. C. o. C. (2001).
582 Idiopathic pulmonary fibrosis: prevailing and evolving hypotheses about its pathogenesis and implications
583 for therapy. *Ann Intern Med*, 134(2), 136-51.

584 Selman, M., Ruiz, V., Cabrera, S., Segura, L., Ramírez, R., Barrios, R., et al. (2000). TIMP-1, -2, -3, and
585 -4 in idiopathic pulmonary fibrosis. A prevailing nondegradative lung microenvironment? *Am J Physiol*
586 *Lung Cell Mol Physiol*, 279(3), L562-74. doi:10.1152/ajplung.2000.279.3.L562.

587 Suga, M., Iyonaga, K., Okamoto, T., Gushima, Y., Miyakawa, H., Akaike, T., et al. (2000). Characteristic
588 elevation of matrix metalloproteinase activity in idiopathic interstitial pneumonias (Research Support,
589 Non-U.S. Gov't). *Am J Respir Crit Care Med*, 162(5), 1949-56. doi:10.1164/ajrccm.162.5.9906096.

590 Urbanski, S. J., Edwards, D. R., Maitland, A., Leco, K. J., Watson, A., & Kossakowska, A. E. (1992).
591 Expression of metalloproteinases and their inhibitors in primary pulmonary carcinomas (Research
592 Support, Non-U.S. Gov't). *Br J Cancer*, 66(6), 1188-94.

593 Wang, Z., Ma, L. J., Kang, Y., Li, X., & Zhang, X. J. (2015). Dickkopf-3 (Dkk3) induces apoptosis in
594 cisplatin-resistant lung adenocarcinoma cells via the Wnt/ β -catenin pathway. *Oncol Rep*, 33(3), 1097-106.
595 doi:10.3892/or.2014.3704.

596 Woessner, J. F., Jr. (1991). Matrix metalloproteinases and their inhibitors in connective tissue remodeling
597 (Research Support, Non-U.S. Gov't
598 Research Support, U.S. Gov't, P.H.S.
599 Review). *FASEB J*, 5(8), 2145-54.

600 Xie, S., Liu, Y., Li, X., Tan, M., Wang, C., Field, J., et al. (2018). Phosphorylation of the Cytoskeletal
601 Protein CAP1 Regulates Non-Small Cell Lung Cancer Survival and Proliferation by GSK3 β . *J Cancer*,
602 9(16), 2825-2833. doi:10.7150/jca.25993.

603 Zhang, L., Wang, Y., Wu, G., Xiong, W., Gu, W., & Wang, C. Y. (2018). Macrophages: friend or foe in
604 idiopathic pulmonary fibrosis? *Respir Res*, 19(1), 170. doi:10.1186/s12931-018-0864-2.

605
606
607

608 **7. Legends to figures**

609 **Figure 1. GSK3 inhibition modulates MMP2 and MMP9 activity.** (a) Densitometric analysis of the
610 intensity of the gelatinolytic bands demonstrated that there was a significant pro-MMP-9 down-
611 modulation by SB216763. Data are given as mean \pm S.D. of three independent animal trials
612 (n=5/treatment) and were normalized to saline values. **, $p < 0.001$ comparing BLM plus SB216763-
613 treated mice with mice given only BLM. (b) Representative gelatin zymography of MMP-9 activity in
614 BALF of mice from each experimental group. BLM-treated mice had two gelatinolytic bands
615 corresponding to NGAL/MMP-9 complex (125 KDa) and pro-MMP-9 (105 KDa). The treatment with
616 SB216763 broke down NGAL/MMP-9 complex and strongly reduced pro-MMP-9. (c) Representative
617 gelatin zymography of MMP-2 activity in BALFs. We detected two gelatinolytic bands corresponding to
618 pro-MMP-2 (72 KDa) and active MMP-2 (52 KDa). (d-e) Densitometric analysis of three independent
619 experiments (n=5/treatment), normalized to saline values for active MMP- and to BLM for pro-MMP-2.
620 Data are shown as mean \pm S.D. * $p < 0.05$, ** $p < 0.001$, comparing BLM plus SB216763-treated mice
621 with mice given only BLM.

622

623 **Figure 2. SB216763 reduced MMP-9, MMP-2, TIMP-1 and TIMP-2 gene overexpression induced**
624 **by BLM.** Real-Time PCR analysis of MMP-9 (a), MMP-2 (b), TIMP-1 (c) and TIMP-2 (d) mRNA
625 extracted from the inflammatory cells of the BALFs. (a) MMP-9 gene expression was strongly induced
626 in BLM-treated mice and SB216763 returned it to the normal levels of the control group. (b) MMP-2
627 expression was augmented in mice following the BLM instillation and the co-treatment with SB216763
628 reduced it. (c) TIMP-1 expression was induced by BLM treatment and SB216763 reduced it to the levels
629 of the normal controls. (d) SB216763 reduced TIMP-2 mRNA levels increased by BLM treatment. Data,
630 presented as *-fold increase*, represent the mean of the ratio of the target mRNA to that of β -actin

631 normalized to the control group (saline) and are expressed as mean \pm S.D. of three independent animal
632 trials. Significance is expressed by * ($p < 0.05$), ** ($p < 0.01$).

633 **Figure 3. GSK-3 inhibition modulates MMPs and TIMPs expression in lung of mice treated with**
634 **bleomycin.** BLM- treated mice show high positivity for MMP-9, TIMP-1, MMP-2 and TIMP-2 in
635 alveolar macrophages (panels a-d). GSK-3 administration down-modulates their expression (panels e-h).
636 Histograms summarize the pathologic scores calculated as the percentage of positive cells for each
637 specific marker. Data are given as mean \pm S.D. of three independent animal trials. * $p < 0.01$ and ** $p <$
638 0.05 . Red arrows: interstitial alveolar macrophages; blue arrow: cuboidalized epithelial alveolar cells.

639 **Figure 4. IHC staining of cuboidalized type II epithelial alveolar cells.** MMP-9, TIMP-1, MMP-2
640 and TIMP-2 were specifically expressed in BLM-treated injured alveolar cells that underwent
641 cuboidalization (panels a-d) and SB216763 selectively reduced their expression (panels e-h).
642 Histograms summarize the effects of GSK-3 inhibition in reducing the BLM-induced epithelial
643 positivity, in particular, for MMP-9 (i) and MMP-2 (j) as showed in the mean \pm S.D of 3 independent
644 animal trials by the histogram. (*) $p < 0.05$.

645 **Figure 5. GSK3 inhibition modulates MMPs activity in-vitro in pulmonary fibroblasts.** MMP2 and
646 MMP9 zymographic analysis of supernatant from MRC5 cells (a,b) and primary IPF fibroblasts (c,d)
647 treated with $\text{TNF}\alpha$ or $\text{TGF}\beta$. SB216763 pretreatment induces a decrease of gelatinolytic activity in
648 MRC5 fibroblasts upon pro-fibrotic stimulation (24 h), both for MMP9 (a) and pro-MMP2 (b). In IPF
649 fibroblasts, instead, SB21 displays no significant effect on MMPs activity (c,d). Data are reported as
650 mean of 3 independent experiments \pm SD. Statistical analysis has been performed by two-tailed t-test
651 and significance is expressed by * ($p < 0,05$), ** ($p < 0,01$).

652

653 **Figure 6. GSK3 inhibition modulates α SMA expression in primary pulmonary fibroblasts.**

654 Western blot analysis of α SMA protein expression in IPF fibroblasts treated with $\text{TNF}\alpha$ or $\text{TGF}\beta$. The
655 increased α SMA expression observed with $\text{TGF}\beta$ is dampened by GSK3 inhibition. Data are reported as
656 mean of 3 independent experiments \pm SD. Statistical analysis has been performed by two-tailed t-test
657 and significance is expressed by * ($p < 0,05$).

658

659 **Figure 7. SB216763 modulates MMP2 protein levels in monocyte-derived cells.** WB analysis of
660 MMP-2 protein levels in primary monocytes/macrophages stimulated with $\text{TNF}\alpha$ or $\text{TGF}\beta$. Both the
661 $\text{TGF}\beta$ -induced increased levels of pro- and active MMP2 proteins are not observed in presence of GSK3
662 inhibitor at the concentration of 2 ng/ml. Data are reported as mean of 3 independent experiments \pm SD.
663 Statistical analysis has been performed by two-tailed t-test and significance is expressed by * ($p < 0,05$).

664

665

666

667

668

669

670

671

672

673

674

675

676 Table 1. Primers used for quantitative real-time PCR

<i>Gene</i>	<i>Forward-primer (3' to 5')</i>	<i>Reverse-primer (3' to 5')</i>	<i>Amplicon length (bp)</i>
β-actin	CTC TCC CTC ACG CCA TCC TG	TCA CGC ACG ATT TCC CTC TCA G	269
MMP-9	CGA CGG CAA GGA CGG C	GTA AGT GGG GAT CAC GAC GC	129
MMP-2	CGG TTT ATT TGG CGG ACA GTG AC	ATT CCC TGC GAA GAA CAC AGC	144
TIMP-1	TGG CAT CCT CTT GTT GCT ATC ACT G	TGA ATT TAG CCC TTA TGA CCA GGT CC	170
TIMP-2	TGC AGA CGT AGT GAT CAG AGC CAA A	AAC TCG ATG TCT TTG TCA GGT CCT T	144

677

678

679

680

681

682

683

684

685

686

687

688

689

690

691

692

693

694

695

In review

696 Table 2. Influence of GSK-3 inhibitor SB216763 on BAL total cell number and cell composition

Experimental groups		total cells (x 10 ⁶)	macrophages (%)	lymphocytes (%)	neutrophils (%)	eosinophils (%)
Saline	n=5/experiment	1.7 ± 0.8	96 ± 1.2	4 ± 3.2	-	-
BLM	n=5/experiment	7.9 ± 4.3 ^ψ	62 ± 4.8	26 ± 7.0	10 ± 6.3	2 ± 1.5
BLM + SB216763	n=5/experiment	2.6 ± 1.8*	87 ± 6.4**	11 ± 6.1*	2 ± 1.5	-

697

In review

Figure 1.JPEG

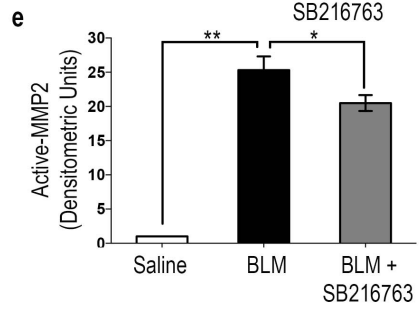
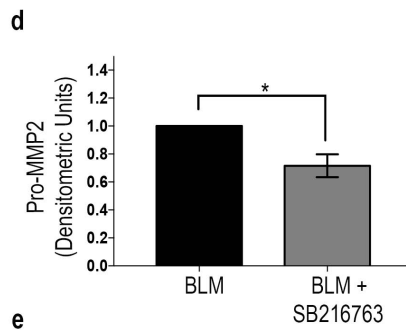
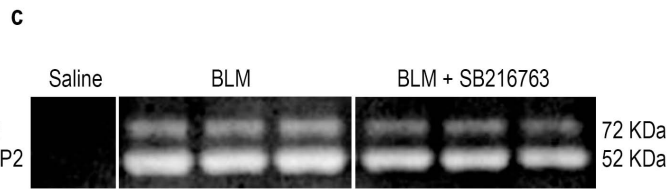
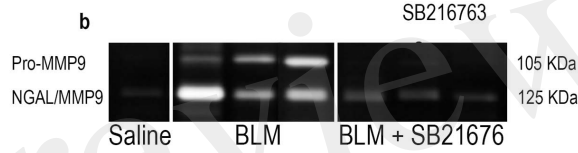
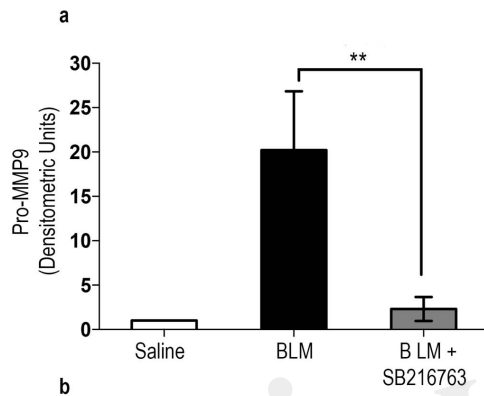


Figure 2.JPEG

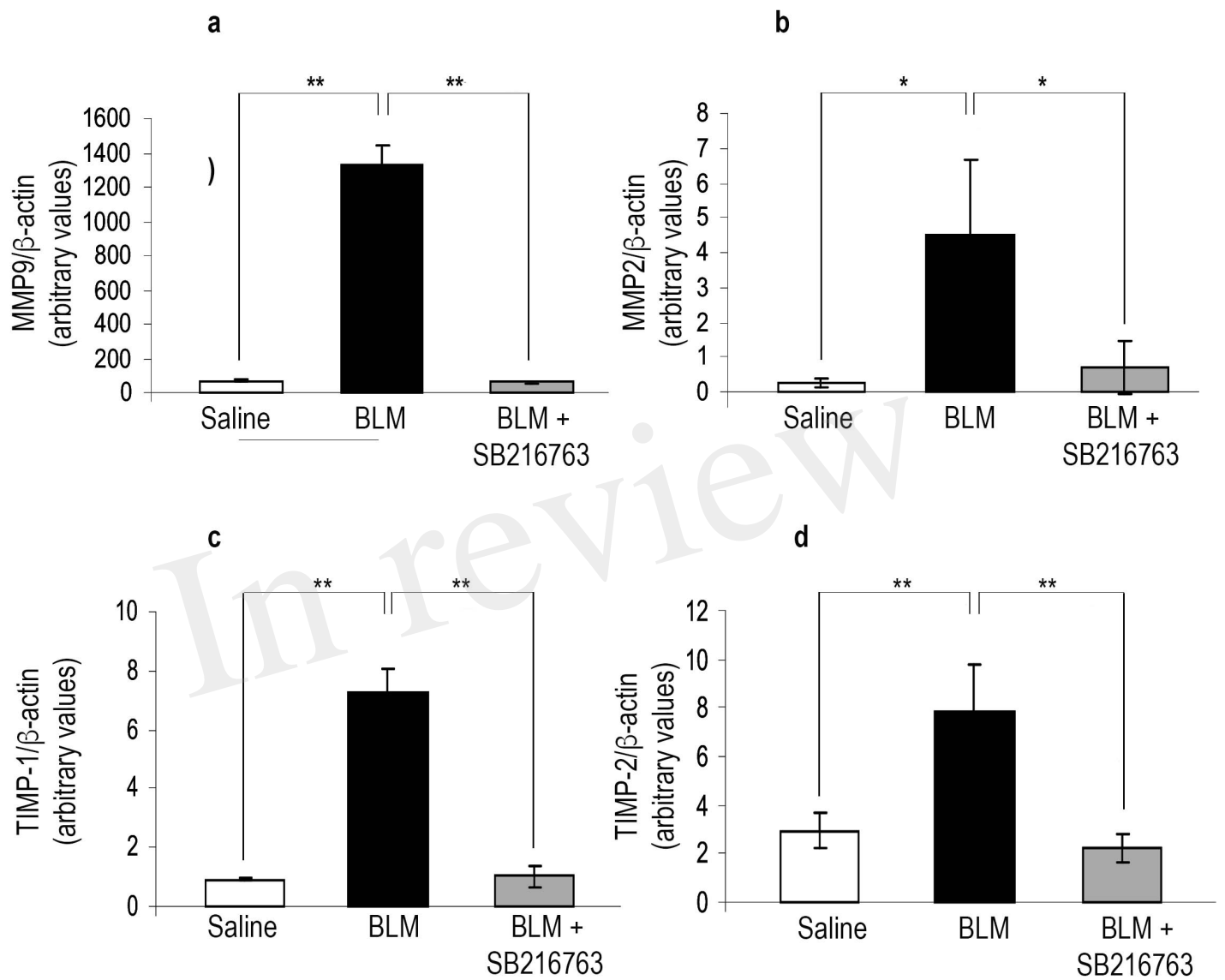


Figure 3.JPEG

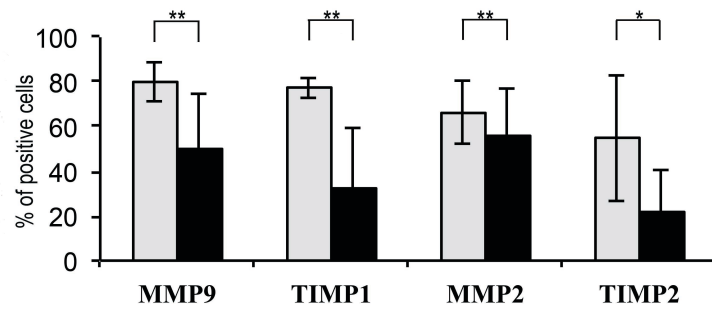
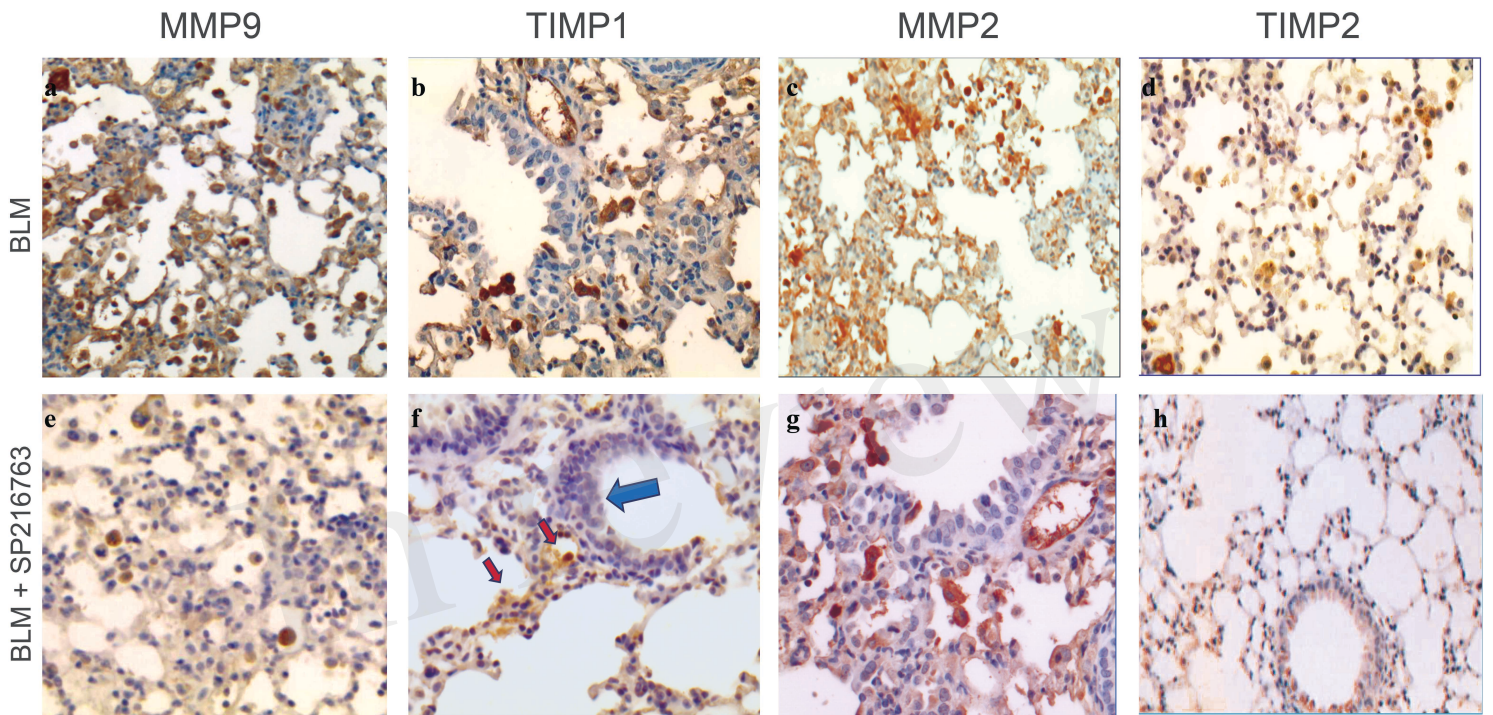


Figure 4.JPEG

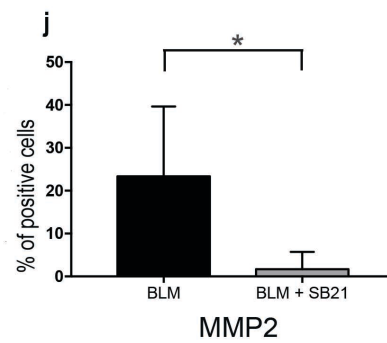
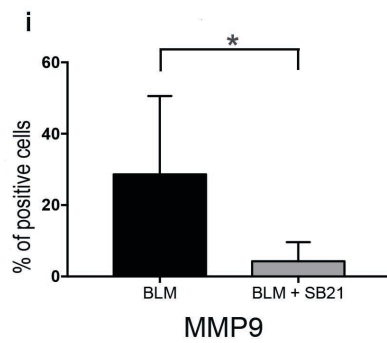
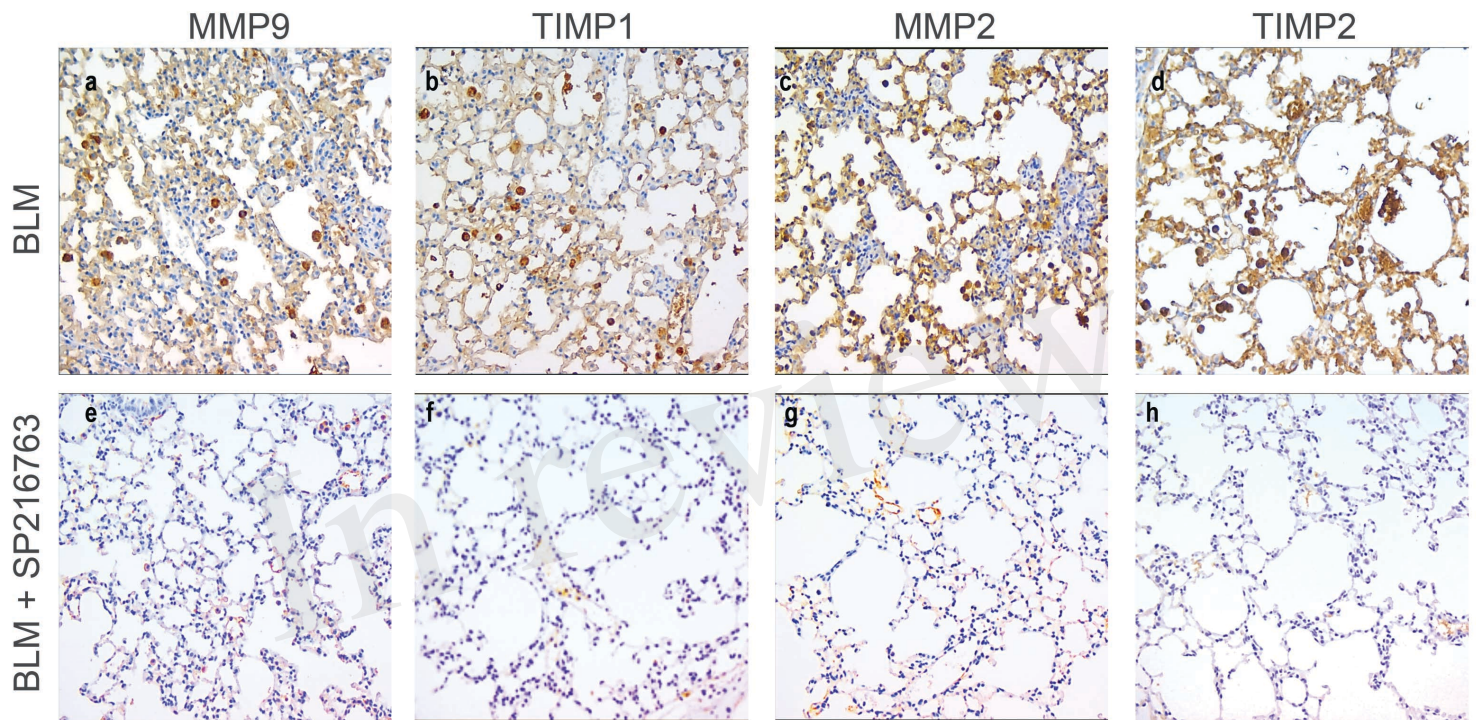


Figure 5.JPEG

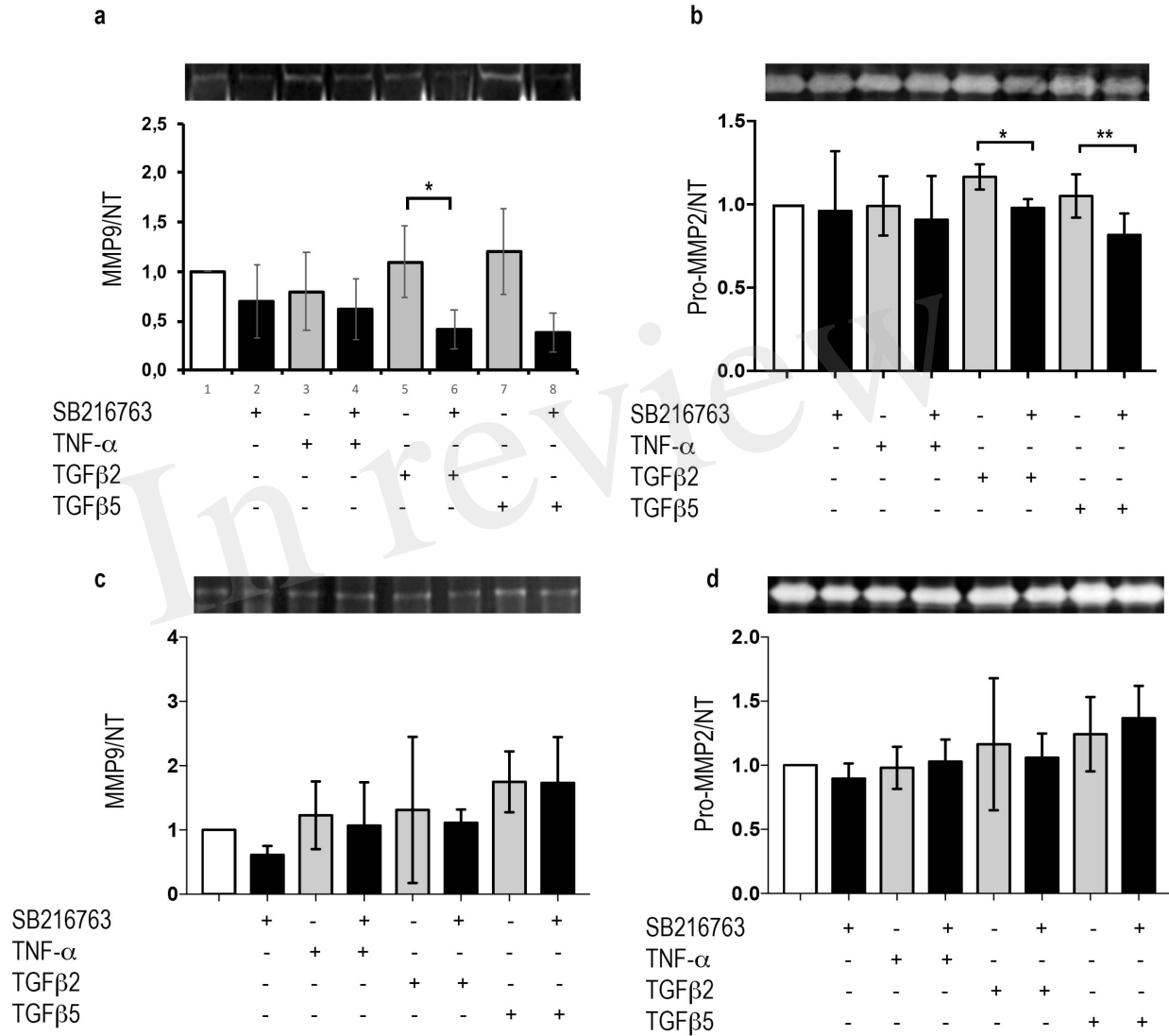


Figure 6.JPEG

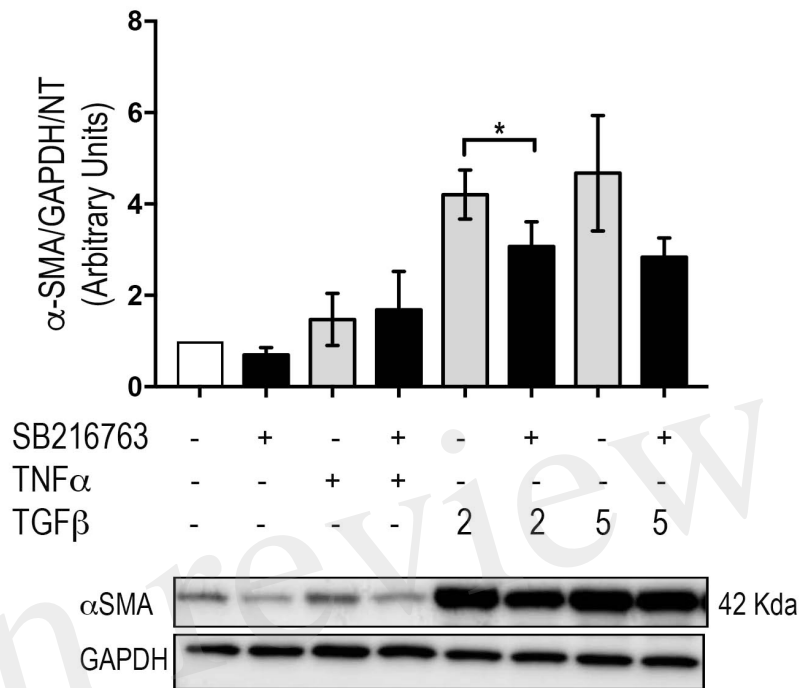


Figure 7.TIF

